Climatic variability in the northern sector of the American tropics since the latest MIS 3

Socorro Lozano-García [a,*], Beatriz Ortega [b], Priyadarsi D. Roy [a], Laura Beramendi-Orosco [a], Margarita Caballero [b]

[a] *Instituto de Geología, Universidad Nacional Autónoma de México, 04510 Mexico City, Mexico*
[b] *Instituto de Geofísica, Universidad Nacional Autónoma de México, 04510 Mexico City, Mexico*

ARTICLE INFO

ABSTRACT

We inferred millennial-scale climate variations and paleohydrological conditions in the northern sector of the American tropics for 30.3–5.5 cal ka BP using geochemical characteristics of sediments from Lake Chalco in central Mexico. The sediment sequence is chronologically constrained with three tephra and nine radiocarbon dates. Temporal variations in titanium, total inorganic carbon, total organic carbon/titanium ratio, carbon/nitrogen ratio, and silica/titanium ratio indicate changes in runoff, salinity, productivity, and sources. Higher concentrations of Ti indicate more runoff during latest Marine Isotope Stage (MIS) 3 (30.3–28.6 cal ka BP). Runoff was lower during the last glacial maximum (LGM; 23–19 cal ka BP) than during the Heinrich 2 event (26–24 cal ka BP). The interval of reduced runoff continued up to 17.5 cal ka BP but increased during the Bølling/Allerød. Trends of decreasing runoff and increasing salinity are observed throughout MIS 1. Lake Chalco received less runoff during the LGM compared to deglaciation, opposite the trend of other North American tropical records. Different amounts of rainfall at different sites are possibly due to shifts in the position of the Intertropical Convergence Zone, changes in the size of the Altlantic warm pool, and varying sea-surface temperatures of the Atlantic and Pacific oceans.

Introduction

The Basin of Mexico (BM) (19°00′–20°00′N; 98°00′–99°30′ W) is located in the northern part of the American tropics (NAT), where modern climate is influenced strongly by the seasonal migration of the Intertropical Convergence (ITCZ). Higher insolation in the Northern Hemisphere and migration of the ITCZ to a more northerly mean position brings precipitation to the region during the boreal summer (Amador et al., 2006). Lakes in the BM receive more runoff during the summer and experience higher water levels. The BM has been an important population center since pre-Columbian times, and numerous archaeological, geological, hydrological, and botanical (Sanders et al., 1979; Niederberger, 1987; Rzedowski and Rzedowski, 2001) studies have provided information about its environmental evolution.

The research of last few decades has extended the knowledge of paleoclimate and paleoecological conditions of this basin to the late Pleistocene. Evidence for glacial advances is preserved in the volcanoes particularly those located in the Sierra Nevada (Telapón, Tlaloc, and Iztaccíhuatl). Vazquez-Selem and Heine (2011) identified at least three different intervals of glacial advance on the Iztaccíhuatl volcano: Hueyatlaco-I between 21 and 17.5 ka, Hueyatlaco-II from 17.5 to 14 ka,

and Milpulco-I during the Younger Dryas (13.5 ka). Lacustrine sediment archives collected from the BM have been studied extensively using multiple biotic and abiotic proxies for paleoenvironmental conditions (Bradbury, 1989, 1997; Lozano-García et al., 1993; Lozano-García and Ortega-Guerrero, 1994, 1998; Caballero-Miranda and Ortega-Guerrero, 1998; Caballero et al., 2010). Most of these studies were carried out on the sediments deposited in the southeastern Lake Chalco sub-basin to understand the limnological evolution (Bradbury, 1989; Caballero-Miranda and Ortega-Guerrero, 1998), vegetation history (Lozano-García et al., 1993; Lozano-García and Ortega-Guerrero, 1994, 1998; Lozano-Garcia, 1996; Correa-Metrio et al., 2013), volcanic activity, tephrachronology and hydrological changes in the region (Ortega-Guerrero and Newton, 1998; Ortega-Guerrero et al., 2000). Recently, it was reported that Lake Chalco preserves a continuous sediment record that covers the last ~200,000 years (Herrera-Hernandez, 2011; Brown et al., 2012).

All these previous studies evaluated the influence of long-term changes in climate, volcanic activity, fire regime, and human impact during the late Pleistocene and Holocene. However, the response to short-term changes, such as the Heinrich events and millennial-scale climate variability, has not been addressed because of relatively poor chronological control in the previously studied sequences.

In this paper, we report geochemical data from a new 1805-cm-long sediment core (CHA VII) (19°15′12.71″N; 98°58′37.68″W) collected from Lake Chalco. Improved chronological control enabled us to outline millennial-scale paleohydrological and other climate variations that

occurred in the basin over the last 30.3 ka. Geochemical characteristics of the sediments provide insight to changes in the amount of terrigenous material delivered by runoff, and shifts in the accumulation of autochthonous organic and inorganic material controlled by productivity and salinity. The proxy records of this sequence are compared with extra-tropical (NGRIP ice core) and other key marine (Cariaco Basin; north of Venezuela) and continental (Juxtlahuaca Cave; southwestern Mexico and Lake Peten Itza; northern Guatemala) paleoclimate records. The response of hydrological balance of the BM to different climate forcings is evaluated by comparison with the summer insolation at 20°N latitude (Wang et al., 2001), temperature variations in the Northern Hemisphere, sea-surface temperatures of the Atlantic and Pacific oceans, and mean position of the ITCZ.

Study site: Basin of Mexico (BM) and Lake Chalco

The BM is one of the high-altitude, inter-montane basins of the Trans-Mexican Volcanic Belt. It was formed during the Neogene by volcanism and tectonism associated with a subduction-related volcanic arc (Ferrari et al., 2012). Formation of the monogenetic Chichinautzin volcanic field at 1.2 Ma led to hydrologic blockage in its southern part, which yielded lacustrine sedimentation (Arce et al., 2013) in five lake systems (Tecocomulco, Xaltocan-Zumpango, Texcoco, Xochimilco, and Chalco) (Fig. 1). The upper ~ 500 m of deposits in several parts of the basin consist of lacustrine sediments (Arce et al., 2013) and provide evidence that significant volcanic activity occurred in the basin and its surroundings. Widely distributed tephra layers have been identified in short cores drilled in Lakes Texcoco and Chalco, and their geochemical characterization and dating allowed the development of a tephrachronological framework for the region (Ortega-Guerrero and Newton, 1998).

Lake Chalco is located in the southern part of the BM at 2200 m a.s.l. and occupies a NNE–SSW-orientated semi-graben. It is an endorheic basin with a catchment area of ~1100 km² that includes the western slopes of Iztaccíhuatl and Popopcatépetl volcanoes (Ortega-Guerrero and Newton, 1998) (Fig. 1). Chalco is surrounded by several volcanic ranges. The Sierra Nevada lies to the east, Chichinautzin volcanic field
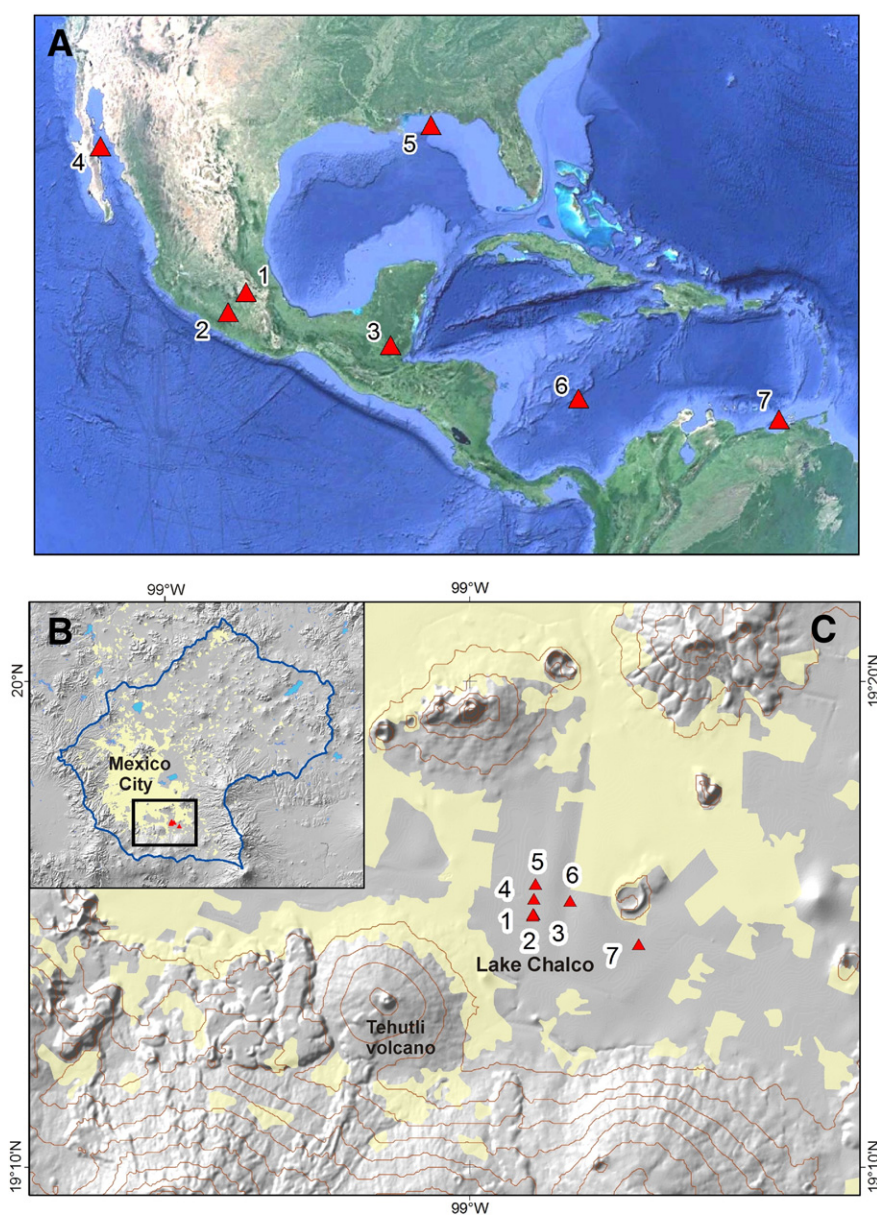
Figure 1. Location maps. (A) North America with the locations of: 1. Lake Chalco in the Basin of Mexico, 2. Juxtlahuaca Cave, 3. Lake Peten Itza, 4. Gulf of California 5. Florida margin, 6. Colombia Basin, 7. Cariaco Basin. (B) Basin of Mexico. Mexico City shown in light yellow. (C) Lake Chalco with the location of the study site (1) core CHA11-VII and previously published Lake Chalco records (2) CHA-08-III; (3) CHA-08-II; (4) CHA-A-B; (5) CHA-C; (6) CHA-D; (7) CHA-E.

to the south, and the Santa Catarina range to the north. The surrounding rocks are volcanic and of intermediate composition (andesite, dacite, basaltic lava flows, and breccia flows) (Ortega-Guerrero et al., 2000). Today, the lake receives average annual precipitation of ~540 mm, mostly during the summer months, and the formerly larger, deeper lake has been reduced to a shallow and marshy ecosystem due to the modern land use changes. The dry season extends from November to March, though occasional rainfall also occurs during the winter months. The annual temperature is ~17°C and the highest temperature is reached during the spring months (27–28.5°C).

Methods

Sampling and analysis

A 1805-cm-long sediment core (CHAVII) was retrieved from the southwestern margin of Lake Chalco (19°30′N, 99°00′ W) using a Usinger coring system. One-meter-long core sections were taken in PVC tubes and sections were split lengthwise and image-scanned at the LacCore facility, University of Minnesota. Chronology of the sequence was based on three tephra layers and eight AMS radiocarbon dates on pollen concentrates and one AMS radiocarbon date on ostracods valves. For the pollen extraction, 2 cm³ of each sample were treated with 1 N HCl (10%), KOH (5%), and HF (100%) (Brown et al., 1989, 1992).

For geochemical analyses, samples were oven-dried at 40°C, homogenized and ground with an agate mortar. Concentrations of Si, Ti, Fe, K, and Ca were measured in 220 samples with a Thermo Scientific NITON FXL 950 X-Ray Fluorescence (XRF) analyzer. Total carbon (TC) and nitrogen (TN) contents were analyzed in 169 samples with a CNHS/O Perkin Elmer 2400 series II elemental analyzer and concentrations of total inorganic carbon (TIC) were measured in a Thermo Scientific HiPerTOC solid analyzer. Total organic carbon (TOC) content was calculated by subtracting TIC from TC. Redundancy analysis was performed using R (R Development Core Team, 2009) to examine co-linearity among the geochemical variables.

Results

Stratigraphy

The core was divided into two stratigraphic units and contains at least five different tephra layers (Fig. 2). Unit II (1805–914 cm, 30.3–27.3 cal ka BP) consists of dark brown to dark gray silt, clay, and sandy silt that is both massive and laminated. Ostracods (1805–1000 cm) and diatoms (1240–950 cm) are common in this unit. Two different tephra layers are present in this unit. A 15-cm-thick tephra is observed at 1725–1710 cm and the Great Basaltic Ash (GBA) (Caballero-Miranda and Ortega-Guerrero, 1998) is present at 1532–1425 cm. Unit I (914–40 cm, 27.3–5.5 cal ka BP) is characterized by black to dark brown silty clay with diatoms, plant remains, and charcoal particles. It has at least three different tephra layers. A 23-cm-thick tephra layer is observed at 570–547 cm; the Tutti Frutti pumice (Sosa-Ceballos et al., 2012) is present at 452–448 cm; and the Upper Toluca Pumice (Arce et al., 2003) is identified at 264–251 cm. The upper 200 cm are characterized by sandy silts and ostracods valves.

Age–depth model

The Bayesian age–depth model (Fig. 2) was constructed with the on-line OxCal version 4.2 (Bronk Ramsey, 2009), after calibrating ages using the IntCal_13 calibration curve (Reimer et al., 2013). The model was based on nine radiocarbon ages (Table 1) and included a P_Sequence with k = 20 (Bronk Ramsey, 2008, 2009). The three tephra deposits in the core (i.e., Great Basaltic Ash, Tutti Frutti Pumice, and Upper Toluca Pumice) were included to be boundaries at their corresponding positions

and were considered to be instantaneous events with no thickness. The Upper Toluca Pumice (UTP) was included using the previously determined date of 10,445 ± 95 ¹⁴C yr BP (12,300 ± 166 cal yr BP) (García-Palomo et al., 2002; Arce et al., 2003). A change in deposition observed at 914 cm depth was also included as a boundary. Results were evaluated in terms of the Agreement Index (A), and the threshold for an acceptable A index is 60% (Bronk Ramsey, 2008). Values are reported as the 95.4% (2σ) posterior probability density intervals with the corresponding median in cal yr BP. The median calibrated age was obtained for every centimeter along the core using the interpolation option of OxCal. Modeled ages are tabulated in Table 1. The resulted Agreement Index for the model was 81%, and for all the samples the agreement yielded results > 72%, indicating an absence of outliers in the sequence. The change in deposition observed at 914 cm depth occurred between 27,530 and 27,200 cal yr BP (median = 27,370 cal yr BP). One result of calibration of the age–depth model was that it yielded an estimated age for the Tutti Frutti Pumice (TFP) of 17,920–17,310 cal yr BP (median = 17,620 cal yr BP), in accordance with the previously reported uncalibrated values, which dated this tephra to 14,500–14,100 ¹⁴C yr BP (17,900–16,900 cal yr BP) (Sosa-Ceballos et al., 2012). The probability density interval estimated with the age–depth model for the GBA gave a date range of 28,960–28,410 cal yr BP (median = 28,690 cal yr BP). These results suggest that the age–depth model is accurate and that the sediment sequence spans the last 30,300 years.

Organic carbon (TOC), inorganic carbon (TIC) and C/N relation

Figure 3 shows concentrations of TOC, TIC, and the C/N ratio in the core. TOC values range between 0.1 and 44.9%. Unit II has lower and relatively homogenous TOC (0.1–8.4%) compared to sediments of Unit I (0.9–44.9%). Highest TOC values are observed at depths of 615–590 cm (18.9–36.4%), 480–444 cm (23.2–29.1%), and 326–272 cm (18.9–44.9%).

Concentrations of TIC vary between 0.2 and 2.4%. TIC is lower in sediments of Unit II (0.2–1.7%) compared to sediments of Unit I (0.2–2.4%). Higher values demarcate the carbonate-enriched sediments at depths of 1613–1595 cm (0.8–1.2%), 1368–956 cm (up to 1.7%) and 171–80 cm (1.3–2.4%). Total nitrogen content (TN) fluctuates from 0.03 to 2.06% and C/N (TOC/TN) varies between 2 and 24. Along the core, variations in TOC content track C/N, i.e. sediments with higher TOC are also characterized by higher C/N. Unit II has C/N values between 2 and 18 and the lower values (<10) are associated with sediments at depths of 1765–1745 cm and 1501–1442 cm. C/N values are higher (11–24) in Unit I and sediments at depths of 605–575 cm, 537–504 cm, and 317–2.82 cm are characterized by C/N > 20.

Elemental geochemistry

Sediments have 19.7–95.0% of Si, 0.1–0.8% of Ti, and 0.3–6.9% of Fe. Ca varies between 0.5 and 11.0% and K shows variations between 0.1 and 1.3% (Fig. 3). Higher concentrations of Si, Ti, Fe, Ca, and K reflect higher abundance of detrital minerals in the sediments. Ca and K, however, can be released from the primary detrital minerals at the sediment–water interface (Mason and Moore, 1982). Similarly, Fe is mobile in anoxic depositional environments (Cohen, 2003). All these elements can re-precipitate as authigenic fractions or be adsorbed onto clay minerals depending on pH-Eh conditions. Ti is insoluble and insensitive to environmental redox variation and represents the abundance of mafic and heavy minerals in the sediments (Mason and Moore, 1982; Yarincik et al., 2000). The positive correlation between Fe and Ti (r = 0.9) suggests that the sources of both the elements are detrital minerals. The relatively lower correlation between K and Ti (r = 0.8) indicates K was partly mobile and possibly adsorbed onto clay minerals. As the core sediments have lacustrine deposits and tephra layers, the detrital minerals originated from erosion of catchment rocks and were products of volcanic activity in the vicinity. Some of the tephra layers, for example, at 1725–1710 cm
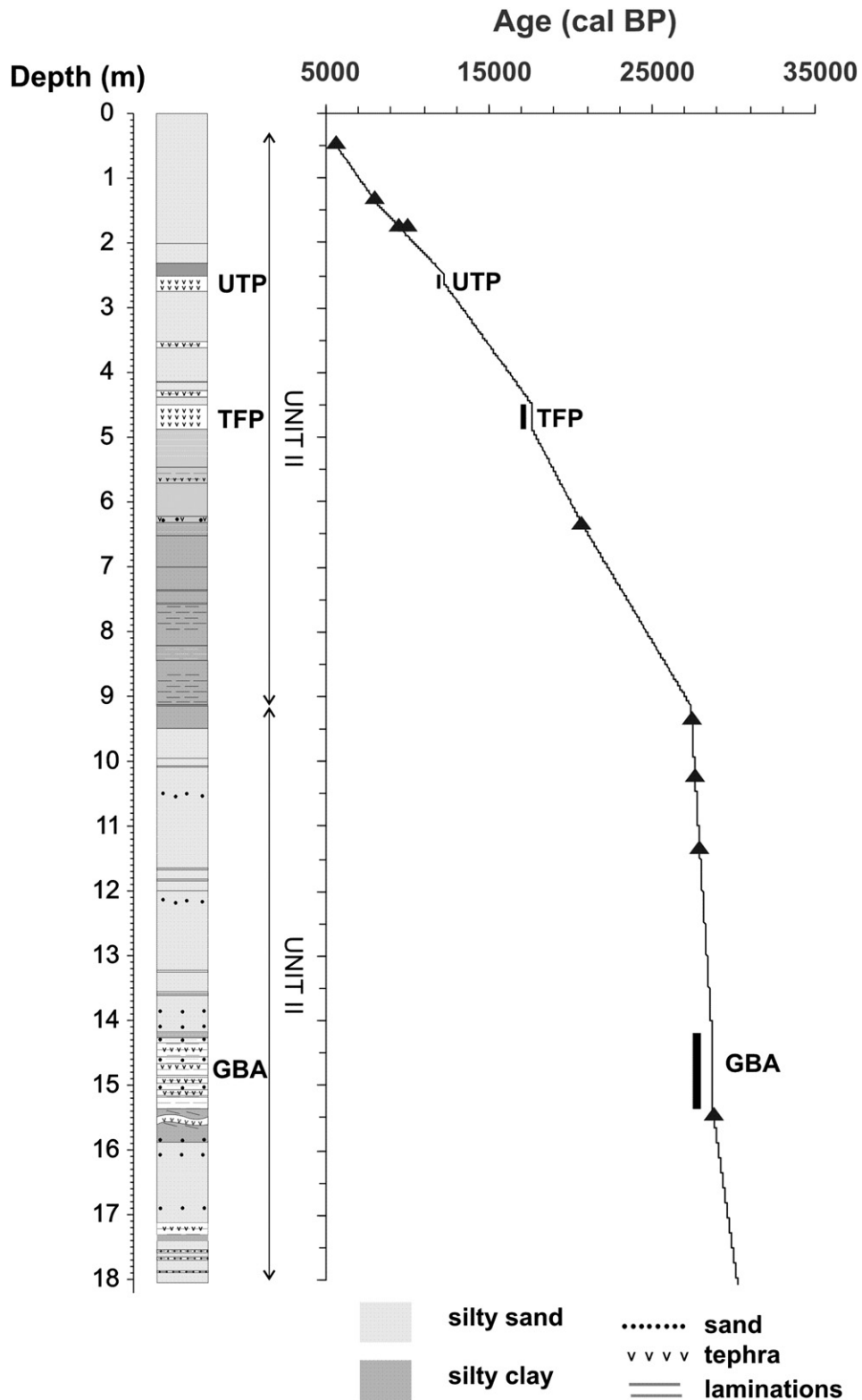
Figure 2. Stratigraphy and age model of Lake Chalco Core CHA VII. Chronology is based on ten AMS ^{14}C dates and three dated tephra layers: Great Basaltic Ash (GBA), Tuti Frutti Pumice (TTP), and Upper Toluca Pumice (UTP).

(GBA) and 570–547 cm, and some sections of the lacustrine deposits without tephra (1800–1535 cm), have higher abundance of Ti.

Correlation between Ca and Ti ($r = 0.3$) is minor and Si shows intermediate correlation with Ti ($r = 0.6$). Higher correlation between Ca and TIC ($r = 0.9$) indicates that higher Ca values are associated with carbonate-enriched sediments. Sediments with greater Si have

intermediate and lower amounts of detrital material, and Si/Ti values distinguish intervals with Si-enriched sediments from those of Ti-enriched sediments. Along the core length, Si/Ti is positively correlated with TOC/Ti ($r = 0.7$). In particular, sediments of 687–611 cm, 525–500 cm, 414 cm, and 121–50 cm are characterized by higher values of both Si/Ti and TOC/Ti (Fig. 3).

Table 1
Radiocarbon ages, boundaries, and calibration results obtained with the Bayesian age–depth model for Chalco core VII.

Sample or parameter	Depth (m)	Material dated	Conventional age (±1σ, 14C yr BP)	Un-modeled calibrated age[a] (2σ, cal yr BP)	Modeled calibrated age[a] (2σ, cal yr BP)	Median (cal yr BP)	Agreement Index (%)
Boundary "end core VII"	n.a.	n.a.	n.a.	n.a.	5650–5470	5560	n.a.
Beta 347500	0.47	pollen	4830 ± 30	5650–5470	5650–5470	5560	97.2
Beta 347502	1.365	ostracods	7220 ± 30	8160–7960	8160–7970	8040	92
Beta 347503	1.375	pollen	7280 ± 40	8180 -8010	8170–8000	8070	97.2
Beta 347501	1.76	pollen	8490 ± 40	9540–9450	9540–9450	9500	99.4
Boundary "UTP"	2.5–2.64	n.a.	10445 ± 95[b]	12610–12020	12590–12000	12300	98.8
Boundary "TuttiFrutti"	4.5–4.88	n.a.	14500 ± 100[c]	17950–17410	17940–17400	17660	n.a.
Beta-359187	6,35	pollen	17180 ± 60	20930–20530	20940–20530	20730	100.6
Boundary "Change"	9.14	n.a.	n.a.	n.a.	27540–27190	27370	n.a.
Beta-359191	9.355	pollen	23180 ± 90	27660–27260	27580–27270	27430	106.4
Beta-359189	10.235	pollen	23450 ± 100	27810–27430	27760–27510	27640	118.4
Beta-359190	11.035	pollen	23720 ± 110	28020–27590	27970–27710	27840	111.3
Boundary "GCB"	14.26–15.32	n.a.	n.a.	n.a.	28970–28410	28690	n.a.
Beta 344189	15.41	pollen	24760 ± 100	29050–28520	29000–28490	28750	100
Boundary "start core VII"	n.a.	n.a.	n.a.	n.a.	31940–28810	30240	n.a.

n.a. not applicable
[a] Calibration using OxCal 4.2 (Bronk Ramsey, 2009) and IntCal_13 radiocarbon calibration curve (Reimer et al., 2013).
[b] Reported by García-Palomo et al. (2002) and Arce et al. (2003).
[c] Reported by Sosa-Ceballos et al. (2012).

Interpretation of paleoenvironmental proxy variables

Variations in Ti, TIC, TOC/Ti, C/N, and Si/Ti were used as proxies for paleohydrological changes. Redundancy analysis shows that the relations between the independent variables and the first two axes explain 70% of the dataset variance (Fig. 4). There is a positive correlation between pairs of elements associated with clastic sediments (i.e., K, Fe, and Ti). Similarly, variables associated with carbonates (i.e., TIC and Ca)
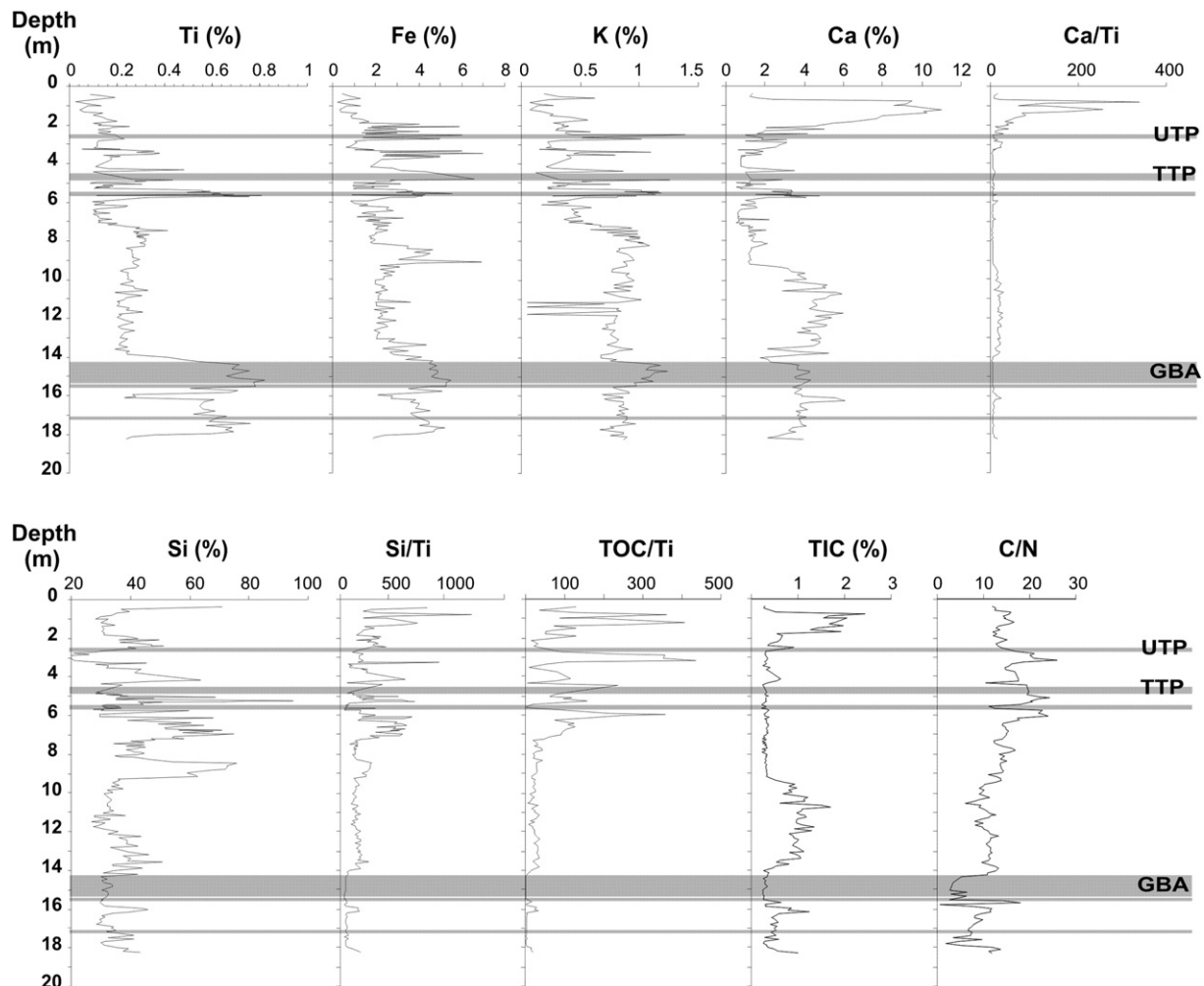
Figure 3. Concentration of Ti, Fe, K, Ca, Si, total organic carbon (TOC), total inorganic carbon (TIC), TOC/Ti ratio and TOC to total nitrogen ratio (C/N) in sediments from Lake Chalco core CHA VII.
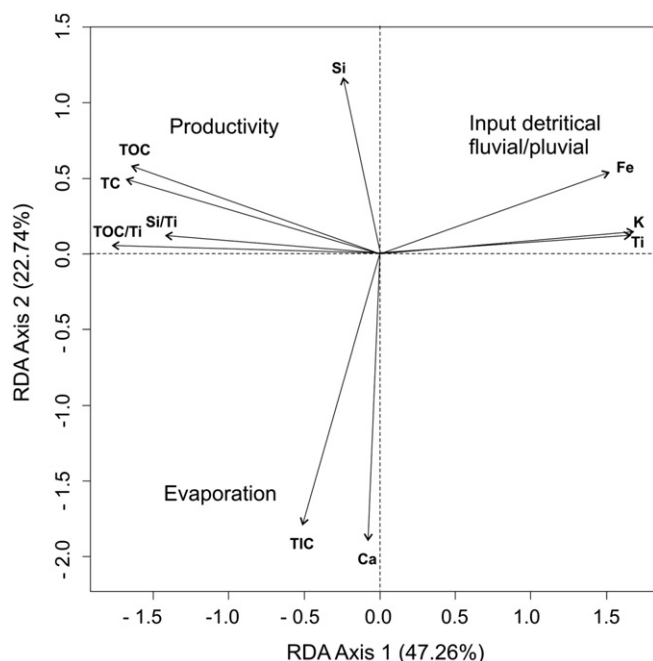
Figure 4. Redundancy analysis of the proxy data from Lake Chalco core CHA VII.

are positively correlated. The Si- and TOC-enriched sediments are positively correlated (i.e., Si/Ti and TOC/Ti).

TIC values represent the abundance of carbonate minerals in bulk sediments. The watershed of Lake Chalco lacks carbonate-bearing rocks and thus the carbonate-enriched sediments were deposited in the basin during the intervals of evaporative conditions and higher salinity. The negative relation between Ti and TIC (r = 0.6) suggests that more Ti-bearing detritals were deposited during the intervals of lower lake-water salinity, i.e. more dilute conditions. Because detrital elements Ti, Fe, and K display similar variations throughout the core, we used only Ti as a proxy to estimate the abundance of pluvially transported detritals and demarcate the intervals of higher runoff into the basin. Except for high values in the main tephra layers at 1718 cm, 1555–1432 cm, 565 cm, 484 cm, and 272 cm (Fig. 3), the sediments with more Ti were deposited during the intervals of higher runoff into Chalco and thus greater precipitation in BM. Previous studies in volcanic basins of Lake Santa Maria del Oro (Sosa-Nájera et al., 2010) and Lake Juanacatlan (Metcalfe et al., 2010) have used the concentration of Ti as a proxy to estimate the dynamics of runoff and precipitation.

TOC content in the bulk sediment was controlled by lacustrine productivity (Cohen, 2003) and influx of clastics into the basin (Katz, 1990). The negative correlation between TOC and Ti (r = −0.5) suggests that intervals of higher clastic influx have a diluting influence on bulk sediment TOC concentration. TOC/Ti eliminates the effect of dilution by clastics and reflects the amount of biomass that sinks to the lake floor. Intervals of more productivity are reflected by sediments with higher values of TOC/Ti. The relative contributions of terrestrial vegetation and lacustrine algae to the lake sediment TOC can be distinguished by the C/N ratio (Meyers and Ishiwatari, 1995). Organic carbon sourced from lacustrine algae has C/N < 10 and the contribution from terrestrial plants increases the C/N values to >10. Sediments with C/N > 20 reflect intervals with a dominant contribution from terrestrial vegetation (Cohen, 2003). Sediments with higher Si have both detrital minerals (i.e., quartz, volcanic glass) and diatoms. As a large part of Si is related to Ti-bearing clastics (r = 0.6), Si/Ti shows the variation of diatom

abundance. Along the core length, Si/Ti is positively correlated with TOC/Ti (r = 0.7) and suggest that the diatom productivity increased during the intervals of enhanced organic productivity. In particular, higher Si/Ti values at 687–611 cm, 525–500 cm, 414 cm, and 121–50 cm are associated with sediments characterized by high TOC/Ti (Fig. 3).

Discussion

Late glacial period

The new geochemical record from Lake Chalco provides paleohydrological information since the latest part of Marine Isotope Stage 3 (MIS 3, 30,300–28,600 cal yr BP) up to the first part of MIS 1 (11, 500–5000 cal yr BP) (Fig. 5). Prior to the volcanic event associated with the GBA tephra, higher values of Ti suggest that the lake received more runoff between 30.3 and 28.6 cal ka BP. C/N values of ≤10 indicate that organic carbon deposited during that interval was mainly sourced from algae. Both the primary productivity and diatom abundance were low in the interval of greater runoff and relatively higher lake stand. Similarly, the water column remained saline even though the lake received more runoff. After the volcanic event at 28.6 cal ka BP, the sediments show an abrupt change to lower Ti values and the trend toward greater evaporation and more saline conditions continued. Productivity indicators show no significant change and the C/N values are comparable to sediments deposited prior to the volcanic event. It is possible that the amount of runoff declined as a consequence of the volcanic activity. GBA tephra has been found in several parts of the BM and its thickness varies from place to place (Lozano-García and Ortega-Guerrero, 1998). The isopach map indicates a southern source for this fallout deposit and it has been proposed that the monogenetic Tehutli volcano, which lies at a distance of ~6.5 km from the core location, could be the source (Ortega Gurerrero et al., in press) (Fig. 1). This volcanic activity might have modified the morphology of the lake and induced a change in the amount of runoff that reached to the southwestern lake margin. TIC values, however, are comparable in sediments deposited before and after the GBA. This suggests that the volcanic event did not cause a change in lake water salinity. There was also no change in total diatom abundance or in the alkaliphilous diatom (*Nitzschia frustulum* and *Cyclotella meneghiniana*) associations before and after the tephra fallout (Caballero-Miranda and Ortega-Guerrero, 1998). In terms of paleovegetation, the basin was dominated by pine forests at the end of MIS 3 (Lozano-Garcia, 1996; Lozano-García and Ortega-Guerrero, 1998).

During the transition from MIS 3 to MIS 2 (~28 cal ka BP), Lake Chalco did not experience any significant change in the amount of runoff. The abrupt decline in TIC values marked the onset of a long-term decrease in temperature and it continued for the next 10 ka. Lower deposition of carbonate minerals was caused by cooler temperature and less evaporation. The C/N values (>10) indicate that lacustrine productivity decreased and terrestrial vegetation contributed more to the sediment organic carbon (Fig. 5). In another sediment core from the same basin, Caballero-Miranda and Ortega-Guerrero (1998) reported an increase in diatom abundance to >30 × 10⁶ valves/gram of dry sediment and a change from alkaliphilous (*Nitzschia frustulum* and *Cyclotella meneghiniana*) to circumneutral taxa (*Cocconeis placentula*) during this cooler interval. Ti values suggest that the change in diatom assemblages and productivity were not related to a significant change in the lake level. We reinterpret the diatom record and consider that the change in diatom assemblage occurred in response to cooler conditions and a change in the physico-chemical characteristics of lake water. The trend towards lower evaporation and less runoff was characterized by a shift from the pine-dominated forests to open juniper forests with grasslands between 27 and 26.5 cal ka BP (Lozano-García and Ortega-Guerrero, 1994; Lozano-García, 1996). In the modern era, open juniper forests with grasslands grow in the drier northern and northeastern sectors of the BM (Rzedowski and Rzedowski, 2001).
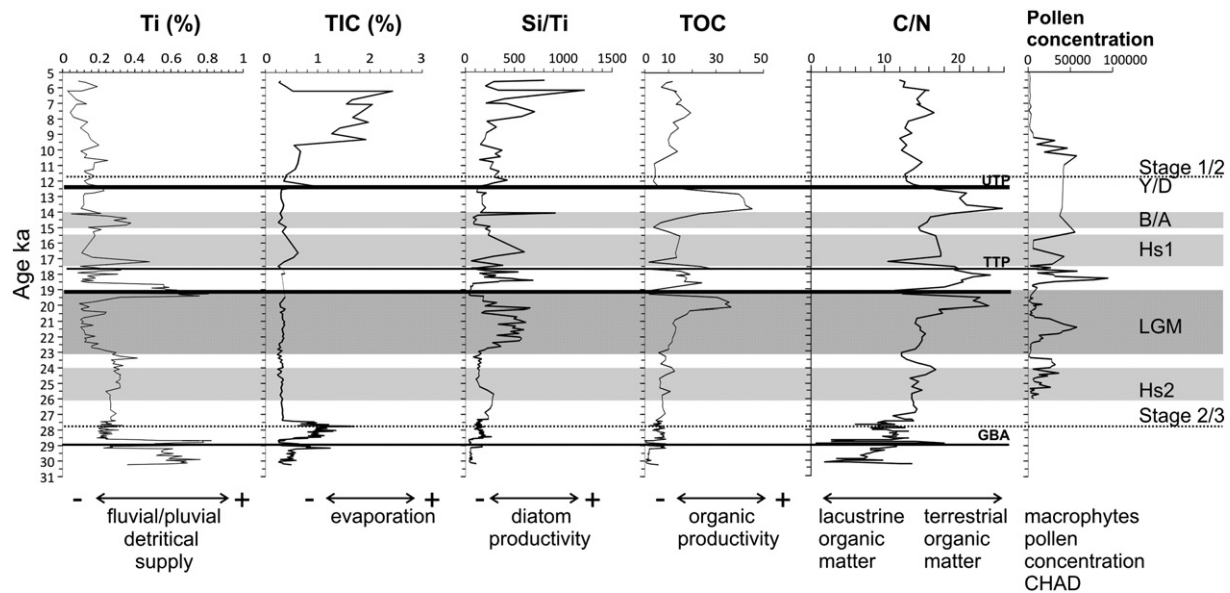
Figure 5. Climate proxy records from Lake Chalco sediments for the past 30.3 cal ka BP. Pluvial/fluvial detrital supply is indicated by Ti% and evaporation is reflected by TIC content. Lacustrine productivity is inferred from the diatom silica to titanium ratio (Si/Ti), total organic carbon (TOC), and organic carbon to total nitrogen ratio (C/N). Expansion of the littoral areas is inferred from the increase in pollen concentration of wetland vegetation in Core CHAD (Lozano-García and Ortega-Guerrero, 1998).

Heinrich event 2 (H2) (26–24 cal ka BP) was characterized by the presence of a shallow and alkaline lake at Chalco. The lake received much less runoff during the LGM (23–19 cal ka BP) than during the H2 event. An extensive glacial advance is reported for Iztaccihuatl Volcano (Hueyatlaco-I) between 21 and 17.5 ka with a 6–8°C reduction in temperature and almost 1000 m lowering of the equilibrium line altitude of the glaciers (3940 m a.s.l.) (Vazquez-Selem and Heine, 2011). Lower lake levels during this cold and dry interval are reflected by an expansion of littoral areas with increase in wetland vegetation indicated by high macrophytes pollen concentrations (Lozano-García et al., 1993; Caballero-Miranda and Ortega-Guerrero, 1998). The diatom record indicates an increase in shallow-water *Eunotia* spp. and Chrysophyte cysts (Fig. 4). Dominance of terrestrial organic matter was observed in the relatively high C/N profile and the maximum contribution from terrestrial vegetation occurred at ~20 cal ka BP.

Deglacial period

Changes in the geochemical characteristics are observed during another volcanic event at 19 cal ka BP. The tephra-dominated sediments are characterized by higher Ti and lower Si/Ti, TOC/Ti, and C/N values. The geochemistry of sediments deposited after this volcanic event are comparable to those of sediments deposited during the LGM. The interval of lower runoff continued up to ~17.5 cal ka BP. Both the higher values of C/N and high abundance of macrophytes pollen indicated expansion of littoral areas. In previous work, Lozano-García (1996) reported development of *Mimosa* scrubland during this dry interval. The H1 event (~17.5–15.5 cal ka BP) was characterized by variable runoff into the Lake Chalco with an abrupt increase in runoff occurring at the beginning of this millennial-scale climate interval. The lake, however, received less runoff and experienced higher diatom and overall primary productivity during the rest of the interval. A slight rise in TIC suggests an increase in the carbonate deposition and relatively warmer conditions. Runoff was higher during the Bølling–Allerød (B/A, ~14.5 cal ka BP) and the diatom assemblage (small *Fragilaria* spp.) also suggests presence of a deeper lake. Multiple geochemical proxies (TIC, Si/Ti, and TOC/Ti) show diluted lake water and less productivity. The C/N ratios complement this interpretation, as macrophytes comprised a smaller fraction of TOC after lake levels increased and the littoral areas were reduced.

Holocene

The shift from MIS 2 to MIS 1 showed evidence of gradually decreasing runoff and increasing abundance of carbonate deposition. This drying trend was recognized in the nearby basin of Santa Cruz Atizapan (Caballero et al., 2002). Warmer conditions and more evaporation during MIS 1 are indicated by the highest TIC values over the early and middle Holocene. The shallow and saline lake water favored a change in diatom assemblages to alkaliphilous, halophilous taxa (*Anomoeoneis costata* and *Amphora veneta*), and a reduction in total diatom abundance. C/N ratios indicate that algal communities became more relevant during ~12–8 cal ka BP. The algal communities provided a smaller contribution to sediment organic carbon after 8 cal ka BP, even as TOC/Ti increased.

Forcings, and comparison with other regional records

The climate of the tropics is controlled by insolation (mostly precession), which modulates changes in mean position of the ITCZ (Wang et al., 2001). Evidence of changes in average position of the ITCZ was inferred from the reflectance of sediments deposited in the Cariaco Basin (Peterson et al., 2000; Haug et al., 2001). It has been proposed that a more southerly positioned ITCZ caused a reduction in the amount of precipitation in the Northern Hemisphere during the cold intervals (stadials and Younger Dryas). On the other hand, a more northerly positioned ITCZ during the warmer periods (interstadials and Holocene) favored more precipitation. During the late glacial period (30.3–19 cal ka BP), while the ITCZ remained at an overall southerly position, the runoff record of Chalco shows positive correlation with orbital-scale variation in summer insolation and with Northern Hemisphere temperatures estimated from the oxygen isotope composition of an ice core from Greenland (Fig. 6). Chalco received more runoff (i.e., more precipitation) during the interval ~30.3–28.6 cal ka BP when the summer insolation was higher and the Northern Hemisphere was warmer. Amount of runoff decreased during the LGM as summer insolation declined and the Northern Hemisphere became cooler. The runoff record is, however, negatively correlated with summer insolation and proxy records for mean position of the ITCZ and Northern Hemisphere temperature over the deglaciation and Holocene. Lake Chalco gradually received less runoff as the higher
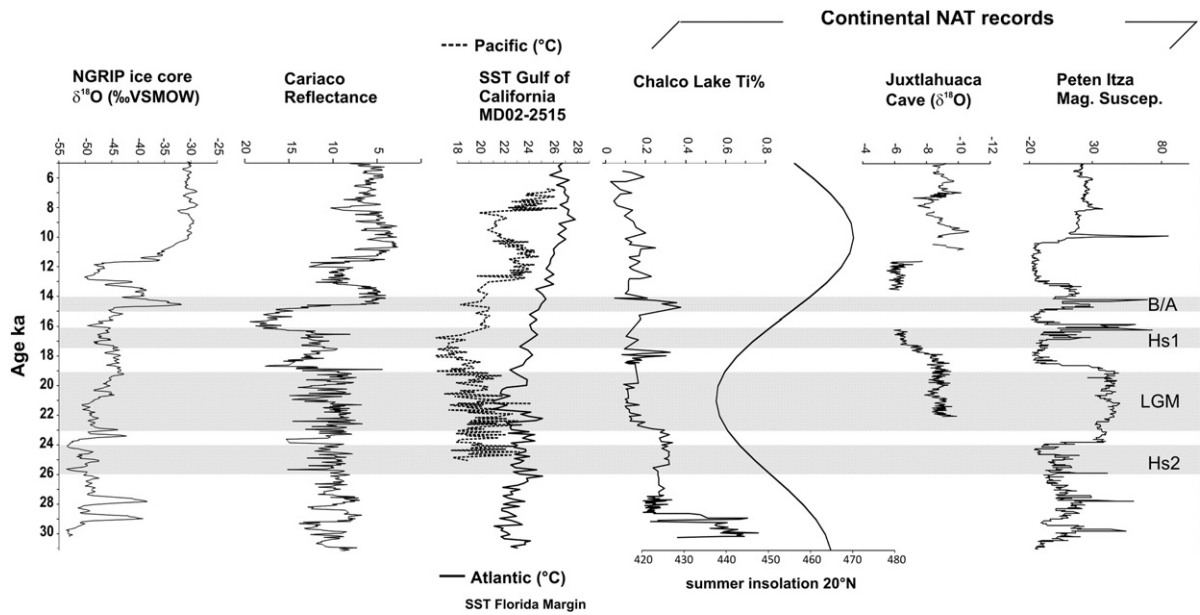
Figure 6. The Lake Chalco Ti record (with Ti concentrations in tephra layers omitted) plotted versus age (cal ka BP), alongside summer insolation at 20° N and other paleoclimate records for the last 30.3 cal ka BP. Millennial oscillations Hs2, LGM, Hs1, and the Bølling–Allerød are indicated with gray shading. Ti data are compared to δ18O of the NGRIP ice core (members, 2004), the Atlantic marine SST records from the Florida margin MD02-2575 (Ziegler et al., 2008), and the Pacific SST record from the Gulf of California MD02-2515 (McClymont et al., 2012). Two continental tropical records are shown, the δ 18O from Juxtlahaca Cave (17°44′ N, 99°16′ W) and the magnetic susceptibility of Lake Peten Itza (16°55′ N, 89°50′ W).

summer insolation shifted the ITCZ to northern latitudes and caused warmer conditions in the Northern Hemisphere.

Comparison of the Lake Chalco Ti record with proxy records of runoff and precipitation from other tropical sites such as Lake Peten Itza (Hodell et al., 2008) and Juxtlahuaca Cave (Lachniet et al., 2013) illustrate that there were different moisture patterns in different parts of the American tropics. Both Lake Peten Itza and Juxtlahuaca Cave (~16–17°N) are located at latitudes south of Lake Chalco (~19°N) and received more precipitation during the LGM compared to the deglaciation. The Peten Itza record also suggests reduction in the amount of precipitation during the H2 event. However, Lake Chalco experienced relatively wetter conditions during the deglaciation in comparison with the LGM. During the H1 event, the two episodes of dry climate separated by an event of wetter and warmer climate in Peten Itza were not detected in the Juxtlahuaca Cave. Registers of sea-surface temperatures (Ziegler et al., 2008; McClymont et al., 2012, Fig. 7) suggest a reduced inter-oceanic pressure gradient between the Atlantic and Pacific during the LGM. This possibly affected the strength of the trade winds and reduced the amount of precipitation in the Basin of Mexico. Increase in the inter-oceanic gradient post-ca.18 cal ka BP could contribute to an enhancement in the precipitation recorded in some of the tropical records. These observations suggest that moisture availability in the American tropics was dominantly controlled by forcings other than the insolation-modulated ITCZ position and North Hemisphere temperature.

In modern times, the available moisture in the American tropics is related to sea-surface temperature and the Atlantic warm pool (AWP) (Wang et al., 2006). The AWP is located along the border of the North Atlantic High pressure subtropical cell (NASH) and spreads over the Caribbean Sea in the east, Gulf of Mexico in the west, and up the eastern coast of North America in the north (Wang et al., 2007). The AWP controls the position, annual variability and strength of the ITCZ and the trade winds that originate at the southern end of the NASH and cross over the Caribbean Sea where their flow intensifies forming the Caribbean low-level jet (Amador et al., 2006). This jet is divided into two branches. The first branch flows westward across Central America into the eastern North Pacific and the second branch flows over the Yucatan Peninsula (Muñoz et al., 2008), moving northward through the Gulf of Mexico to join with the southerly Great Plains low level jet (GPLLJ) (Wang et al., 2008). The second branch transports moisture from the

Atlantic and the Caribbean to central Mexico. Today, it is deflected northwards by the low pressure established over the central-eastern USA and provides moisture to the central USA.

The annual and interannual variability of the AWP has an important effect on the amount of moisture transported (Wang et al., 2007). Proxy records of sea-surface temperatures from the Florida margin (Ziegler et al., 2008), Cariaco Basin (Lea et al., 2003), and Colombia Basin (Schmidt et al., 2004) provide information about the size and location
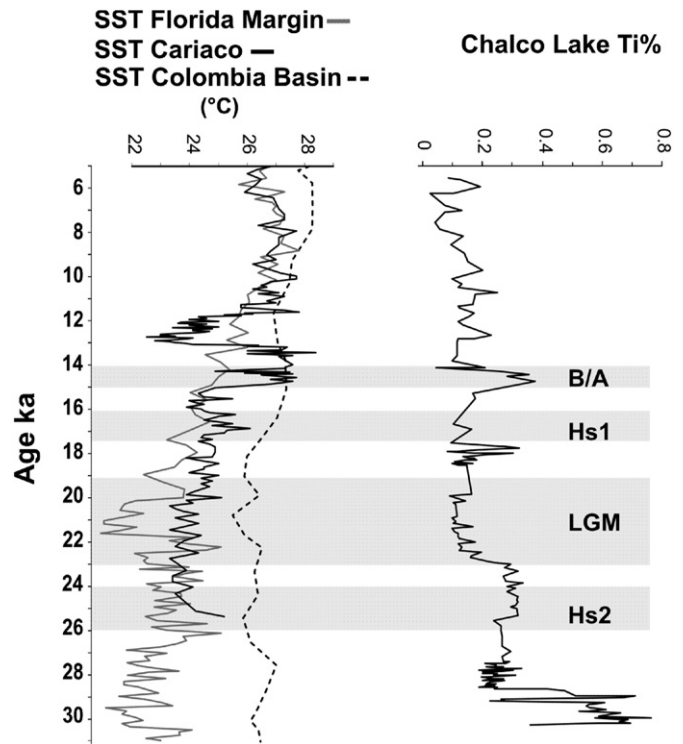
Figure 7. The Lake Chalco Ti (%) record and the sea-surface temperatures records from the Florida margin MD02-2575 (Ziegler et al., 2008), the Cariaco Basin PL7-39PC (Lea et al., 2003), and the Colombia Basin ODP 999A/VM28-122 (Schmidt et al., 2004).

of the AWP during the late glacial period and Holocene (Fig. 7). During the late glacial period and LGM, the Florida margin in the Gulf of Mexico was as much as ~6°C cooler compared to the Colombia Basin, and the Cariaco Basin was as much as ~3°C cooler compared to the Colombia Basin. Weak Atlantic meridional overturning circulation (AMOC) during this interval of restricted AWP caused transportation of moisture into the sites located at lower latitudes, such as Juxtlahuaca and Peten Itza. Over the deglaciation, Chalco received more runoff during the initial part of the H1 event and during the B/A. During both events, the Cariaco Basin and Colombia Basin had the lowest temperature differences and both basins were warmer compared to the Florida margin. During this interval with an intermediate-size AWP, more moisture reached Peten Itza by one branch and central Mexico received more precipitation by the other branch. We relate the arid conditions at Juxtlahuaca Cave to cooler conditions in the Pacific Ocean, estimated from an alkenone-based proxy record from the Gulf of California (McClymont et al., 2012).

During the Holocene (MIS 1), sea-surface temperatures in the Cariaco Basin and Florida margin were similar and the temperature difference with the Colombia Basin was lowest. This suggests that the AWP included the Gulf of Mexico and reached its maximum size. Reduced runoff into Lake Chalco, increased runoff into Lake Peten Itza, and more precipitation at Juxtlahuaca Cave all suggest that the branch transporting moisture across Central America remained stronger. The other branch, transporting moisture from the Atlantic and the Caribbean into central Mexico, was deflected northward by the low pressure established over the central-eastern USA by more summer insolation, and provided moisture into the central USA. In general, the sea-surface temperature record of the Gulf of California (McClymont et al., 2012) indicated warmer conditions in the Pacific Ocean during this interval, and Juxtlahuaca Cave received additional moisture from the Pacific Ocean.

Conclusions

Geochemistry of Lake Chalco sediment provides a continuous record of paleohydrological changes from the northern neotropical highlands between 30.3 and 5.5 cal ka BP. The millennial-scale hydrological variations in the central Mexican highlands were identified using elemental concentrations, total organic and inorganic carbon data, and the C/N ratio.

1. Precipitation was more in conjunction with higher insolation in the latest part of MIS 3 (30.3–28.6 cal ka BP). Enhanced inflow into the basin and diluted lake water column were indicated by highest Ti along with lower TIC.
2. The transition from MIS 3 to MIS 2 (ca. 27.8 cal ka BP) was characterized by reduced TIC values. This trend, indicating less evaporation and colder temperatures, lasted for the next 10 cal ka BP.
3. Summer insolation remained lower over MIS 2, and a reduction in the amount of precipitation during the LGM caused lower runoff into Chalco. The contribution of terrestrial vegetation and macrophyte pollen on total productivity increased. This interval of reduced runoff continued from the LGM up to the initiation of the deglacial period (17.5 ka).
4. Runoff was variable during the H1 event and moister conditions prevailed during the Bølling/Allerød. A trend towards less humidity with lower runoff and warmer conditions was observed during the first part of MIS 1.
5. Lake Chalco received less runoff during the LGM compared to the deglaciation. This trend is opposite of other paleoclimatic records from the region (e.g., Juxtlahuaca Cave and Lake Peten Itza). This complex nature of late glacial climate variability suggests that the north–south shifts of the ITCZ (causing wet/dry conditions in the region) is insufficient to explain the tropical precipitation variability. Other forcings, such as the Atlantic warm pool and temperature gradient between the Atlantic and Pacific oceans, were involved. The documentation

of the climate responses at multiple sites is critical to understand the climate changes we face today.

References

Amador, J.A., Alfaro, E.J., Lizano, O.G., Magaña, V.O., 2006. Atmospheric forcing of the eastern tropical Pacific: a review. Journal of Climate 69, 101–142.

Arce, J.L., Macías, J.L., Vázquez-Selem, L., 2003. The 10.5 ka plinial eruption of Nevado de Toluca, Mexico, stratigraphical and hazard implications. Geological Society of America Bulletin 115, 230–248.

Arce, J.L., Layer, P.W., Lassiter, J.C., Benowitz, J.A., Macías, J.L., Ramírez-Espinosa, J., 2013. 40Ar/39Ar dating, geochemistry, and isotopic analyses of the quaternary Chichinautzin volcanic field, south of Mexico City: implications for timing, eruption rate, and distribution of volcanism. Bulletin of Volcanology 75, 774.

Bradbury, J.P., 1989. Late Quaternary lacustrine paleoenvironments in the Cuenca of Mexico. Quaternary Science Reviews 8, 75–100.

Bradbury, J.P., 1997. Sources of glacial moisture in Mesoamerica. Quaternary International 43 (44), 97–110.

Bronk Ramsey, C., 2008. Deposition models for chronological records. Quaternary Science Reviews 27, 42–60.

Bronk Ramsey, C., 2009. Bayesian analysis of radiocarbon dates. Radiocarbon 51, 337–359.

Brown, T.A., Nelson, D.E., Mathewes, R.W., Vogel, J.S., Southon, J.R., 1989. Radiocarbon dating of pollen acelerator mass spectrometry. Quaternary Research 32, 205–212.

Brown, T.A., Farwell, G.W., Grootes, P.M., Schmidt, F.H., 1992. Radiocarbon AMS dating pollen extracted peat samples. Radiocarbon 34, 550–556.

Brown, E.T., Werne, J.P., Lozano-García, M.S., Caballero, M., Ortega-Guerrero, B., Cabral-Cano, E., Valero-Garces, B.L., Schwalb, A., Arciniega-Ceballos, A., 2012. Scientific drilling in the Basin of Mexico to evaluate climate history, hydrological resouces, and siesmic and volcanic hazards. Scientific Drilling 14, 72–75.

Caballero, M., Ortega, B., Valadez, F., Metcalfe, S.E., Macias, J.L., Sugiura, Y., 2002. Sta. Cruz Atizapán: a 22-ka lake level record and climatic implicatios for the late Holocene human occupation in the Upper Lerma Basin, Central Mexico. Palaeogeography, Palaeoclimatology, Palaeoecology 186, 217–235.

Caballero, M., Ortega-Garcia, M.S., Vazquez-Selem, L., Ortega, B., 2010. Evidencias de cambio climático y ambiental en los registros glaciales y en cuencas lacustres del centro de México durante el último máximo glacial. Boletín de la Sociedad Geológica Mexicana 62, 359–377.

Caballero-Miranda, M., Ortega-Guerrero, B., 1998. Lake levels sice about 40,000 years ago at Lake Chalco, near Mexico City. Quaternary Research 50, 69–79.

Cohen, A.S., 2003. Palaeolimnology: the history and evolution of lake systems. Oxford University Press, New York.

Correa-Metrio, A., Bush, M.B., Lozano-Garcia, S., Sosa-Nájera, S., 2013. Millennial-scale temperature change velocity in the continental northern Neotropics. PLoS ONE 8, e81958.

Ferrari, L., Orozco-Esquivel, M.T., Manea, V., Manea, M., 2012. The dynamic history of the Trans-Mexican Volcanic Belt and the Mexico subduction zone. Tectonophysics 522–523, 122–149.

García-Palomo, A., Macías, J.L., Capra, L., 2002. Geology of Nevado de Toluca Volcano and surrounding areas, central Mexico. Map and Chart Series MCH089. Geological Society of America, p. 26.

Haug, G.H., Hughen, K.A., Sigman, D.M., Peterson, L.C., Rohl, U., 2001. Southward migration of the Intertropical Convergence Zone through the Holocene. Science 293, 1304–1308.

Herrera-Hernandez, D., 2011. Estratigrafía y análisi de facies de los sedimentos lacustres del Cuaternario tardío de la cuenca de Chalco, México. Instituto de Geofísica Universidad Nacional Autónoma de México, p. 122.

Hodell, D.A., Anselmetti, F.S., Aristegui, D., Brenner, M., Curtis, J.H., Gilli, A., Grzesik, A., Guilderson, T.J., Müller, A.D., Bush, M.B., Correa-Metrio, A., Escobar, J., Kutterolf, S., 2008. An 85-ka record of climate change in lowland Central America. Quaternary Science Reviews 27, 1152–1165.

Katz, B.J., 1990. Controls on the distribution of lacustrine source rocks through time and space. In: Katz, B.J. (Ed.), Lacustrine Basin Exploration: Case Studies and Modern Analogues. American Association of Petroleum Geologists, pp. 61–76.

Lachniet, M.S., Asmeron, Y., J.P.,B., Polyak, V.J., Vazquez-Señem, L., 2013. Orbital pacing and ocean circulation-induced collapses of the Mesoameican monsoon over the past 22,000 y. PNAS 110, 9255–9260.

Lea, D.W., Pak, D.K., Peterson, L.C., Hughen, K.A., 2003. Synchroneity of tropical and high-latitude atlantic temperatures over the last glacial termination. Science 301, 1361–1364.

Lozano-García, M.S., 1996. La vegetación Cuaternaria en el Centro de México: Registros Palinológicos e Implicaciones Paleoclimáticas. Boletín de la Sociedad Botánica de México 109.

Lozano-Garcia, S., 1996. La vegetación Cuaternaria en el Centro de México: Registros Palinológicos e Implicaciones Paleoclimáticas. Boletín de la Sociedad Botánica de México 57, 79–102.

Lozano-García, M.S., Ortega-Guerrero, B., 1994. Palynological and magnetic susceptibility records of Lake Chalco, central Mexico. Palaeogeography, Palaeoclimatology, Palaeoecology 109, 177–191.

Lozano-García, M.S., Ortega-Guerrero, B., 1998. Late Quaternary environmental changes of the central part of the Basin of Mexico: correlation between Texcoco and Chalco basins. Review of Palaeobotany and Palynology 99, 77–93.

Lozano-García, M.S., Ortega-Guerrero, B., Caballero-Miranda, M., Urrutia-Fucugauchi, J., 1993. Late Pleistocene and Holocene paleoenvironments of Chalco Lake, Central Mexico. Quaternary Research 40, 332–342.

Mason, B., Moore, C.B., 1982. Principles of Geochemistry. John Wiley & Sons, New York.

McClymont, E.L., Ganeshram, R.S., Pichevin, L.E., Talbot, H.M., van Dongen, B.E., Thunell, R.C., Haywood, A.M., Singarayer, J.S., Valdes, P.J., 2012. Sea-surface temperature records of Termination 1 in the Gulf of California: challenges for seasonal and interannual analogues of tropical Pacific climate change. Paleoceanography 27. http://dx.doi.org/10.1029/2011PA002226.

Metcalfe, S.E., Jones, M.D., Davies, S.J., Noren, A., MacKenzie, A.B., 2010. Climate variability over the last two millennia in the North American Monsoon region, recorded in laminated lake sediments from Laguna de Juanacatlán, Mexico. The Holocene 20, 1195–1206.

Meyers, P.A., Ishiwatari, R., 1995. Organic matter accumulation records in lake sediments. In: Lerman, A., Imboden, D., Gat, J. (Eds.), Physics and Chemistry of Lakes. Springer-Verlag, New York, pp. 279–328.

Muñoz, E., Busalacchi, A.J., Nigam, S., Ruiz-Barradas, A., 2008. Winter and summer structure of the Caribbean low-level jet. Journal of Climate 21, 1260–1276.

Niederberger, C., 1987. Paleopaysages et archeologie pre-urbaine du basin de Mexico. Centr d'etudes Mexicaines et Centamericaines, Mexico.

Ortega-Guerrero, B., Lozano-García, S., Caballero, M., 2015. Historia de la evolución deposicinal del lago de Chalco, México desde el MIS 3. Boletín de la Sociedad Geológica Mexicana (in press).

Ortega-Guerrero, B., Newton, A.J., 1998. Geochemical characterization of Late Pleistocene and Holocene tephra layers from the Basin of Mexico, Central Mexico. Quaternary Research 50, 90–106.

Ortega-Guerrero, B., Thompson, R., Urrutia-Fucugauchi, J., 2000. Magnetic properties of lake sediments from Lake Chalco, central Mexico, and their palaeoenvironmental implications. Journal of Quaternary Science 15, 127–140.

Peterson, L.C., Haug, G.H., Hughen, K.A., Röhl, U., 2000. Rapid changes in the hydrologic cycle of the Tropical Atlantic during the Last Glacial. Science 290, 1947–1951.

R Development Core Team, 2009. R: A language and environment for statistical computing. 2.10 ed. R Foundation for Statistical Computing, Vienna, Austria 3-900051-07-0 (http://www.R-project.org).

Reimer, P.J., Bard, E., Bayliss, A., Beck, J.W., Blackwell, P.G., Bronk Ramsey, C., Buck, C.E., Cheng, H., Edwards, R.L., Friedrich, M., Grootes, P.M., Guilderson, T.P., Haflidason, H., Hajdas, I., Hatté, C., Heaton, T.J., Hoffmann, D.L., Hogg, A.G., Hughen, K.A., Kaiser, K.F., Kromer, B., Manning, S.W., Niu, M., Reimer, R.W., Richards, D.A., Scott, E.M., Southon, J.R., Staff, R.A., Turney, C.S.M., van der Plicht, J., 2013. IntCal13 and Marine13 Radiocarbon Age Calibration Curves 0–50,000 Years cal BP. Radiocarbon 55, 1869–1887.

Rzedowski, G.C., Rzedowski, J., 2001. Flora fanerogámica del Valle de México Instituto de Ecología. A.C. y Comisión Nacional para el Conocimiento y Uso de la Biodiversidad.

Sanders, W.T., Parsons, J.R., Stantley, R.S., 1979. The basin of Mexico. Ecological processes in the evolution of a civilization. Academic Press.

Schmidt, M.W., Spero, H.J., Lea, D.W., 2004. Links between salinity variation in the Caribbean and North Atlantic thermohaline circulation. Nature 428, 160–163.

Sosa-Ceballos, G., Gardner, J.E., Siebe, C., Macías, J.L., 2012. A caldera-forming eruption ~14100 14C yr BP at Popocatépetl volcano, México. Insights from eruption dynamics and magma mixing. Journal of Volcanology and Geothermal Research 212–213, 27–40.

Sosa-Nájera, S., Lozano-García, M.S., Roy, P.D., Caballero, M., 2010. Registro de sequías históricas en el occidente de México con base en el análisis elemental de sedimentos lacustres: El caso del lago Santa María del Oro. Boletín de la Sociedad Geológica Mexicana 62, 437–451.

Vazquez-Selem, L., Heine, K., 2011. Late Quaternary Glaciation in Mexico. In: Ehlers, J., Gibbard, P.L. (Eds.), Quaternary Glaciations - Extent and Chronology, Part III: South America, Asia, Africa, Australia, Antarctica. Elsevier, Amsterdam, pp. 233–242.

Wang, Y.J., Cheng, H., Edwards, R.L., An, Z.S., Wu, J.Y., Shen, C.C., Dorale, J.A., 2001. A high-resolution absolute-dated late Pleistocene monsoon record from Hulu cave, China. Science 294, 2345–2348.

Wang, C., Enfield, D.B., Lee, S.K., Landsea, C.W., 2006. Influences of the Atlantic Warm pool on Western Hemisphere summer rainfall and Atlantic hurricanes. Journal of Climate 19, 3011–3028.

Wang, C., Lee, S., Enfield, B.D., 2007. Impact of the Atlantic warm pool on the summer climate of the western hemisphere. Journal of Climate 20, 50215040.

Wang, C., Lee, S.-L., Enfield, D.B., 2008. Atlantic warm pool acting as a link between atlantic multidecadal oscillation and atlantic tropical cyclone activity. Geochemistry, Geophysics, Geosystems 9, Q05V03.

Yarincik, K.M., Murray, R.W., Lyons, T.W., Peterson, L.C., Haug, G.H., 2000. Oxygenation history of bottom waters in the Cariaco Basin, Venezuela, over the past 578,000 years: Results from redox-sensitive metals (Mo, V, Mn, and Fe) (Paper 1999PA000401). Paleoceanography 15, 593–604.

Ziegler, M., Nürnberg, D., Karas, C., Tiedemann, R., Lourens, J.L., 2008. Persistent summer expansion of the Atlantic warm pool during glacial abrupt cold events. Nature Geoscience 1, 601–605.